

OPEN ACCESS

**Repository of the Max Delbrück Center for Molecular Medicine (MDC)
in the Helmholtz Association**

<http://edoc.mdc-berlin.de/16155>

Mouse model for acute Epstein-Barr virus infection

Wirtz, T. and Weber, T. and Kracker, S. and Sommermann, T. and Rajewsky, K. and Yasuda, T.

This is the final version of the accepted manuscript. The original article has been published in final edited form in:

Proceedings of the National Academy of Sciences of the United States of America
2016 NOV 29 ; 113(48): 13821-13826
2016 NOV 16 (first published online)
doi: [10.1073/pnas.1616574113](https://doi.org/10.1073/pnas.1616574113)

Publisher: [National Academy of Science](#)

© 2016 The Author(s)

A mouse model for acute Epstein-Barr virus infection

Tristan Wirtz^{1,a}, Timm Weber^{1,a}, Sven Kracker^{2,3}, Thomas Sommermann¹, Klaus Rajewsky^{1,2,b}, and Tomoharu Yasuda^{1,2,b}

¹ Immune Regulation and Cancer, Max Delbrück Center for Molecular Medicine, 13125 Berlin, Germany.

² Program in Cellular and Molecular Medicine, Children's Hospital and Immune Disease Institute, Harvard Medical School, Boston, MA 02115, USA.

³ Université Paris Descartes, Sorbonne Paris Cité, Imagine Institute, INSERM UMR 1163, Human Lymphohematopoiesis Laboratory, Paris, France.

^a T.Wi. and T.We. contributed equally to this work.

^b Correspondence: tomoharu.yasuda@mdc-berlin.de and klaus.rajewsky@mdc-berlin.de

Keywords: Epstein-Barr virus, LMP1, LMP2A, Familial hemophagocytic lymphohistiocytosis, Post-transplant lymphoproliferative disorder.

Abstract

Epstein-Barr Virus (EBV) infects human B cells and drives them into continuous proliferation. Two key viral factors in this process are latent membrane proteins LMP1 and LMP2A, which mimic constitutively activated CD40 receptor and B cell receptor (BCR) signaling, respectively. EBV-infected B cells elicit a powerful T cell response which clears the infected B cells and leads to life-long immunity. Insufficient immune surveillance of EBV-infected B cells causes life-threatening lymphoproliferative disorders, including mostly germinal center (GC)-derived B cell lymphomas. We have modeled acute EBV infection of naïve and GC B cells in mice, through timed expression of LMP1 and LMP2A. While lethal when induced in all B cells, induction of LMP1 and LMP2A in just a small fraction of naïve B cells initiated a phase of rapid B cell expansion followed by a proliferative T cell response, clearing the LMP-expressing B cells. Interfering with T cell activity prevented clearance of LMP-expressing B cells. This was also true for perforin deficiency, which in the human causes a life-threatening EBV-related

immunoproliferative syndrome. LMP expression in GC B cells impeded the GC reaction but, upon loss of T cell surveillance, led to fatal B cell expansion. Thus, timed expression of LMP1 together with LMP2A in subsets of mouse B cells allows one to study major clinically relevant features of human EBV infection *in vivo*, opening the way to new therapeutic approaches.

Significance

Epstein-Barr Virus infects human B cells and drives them into proliferation and transformation. While more than 90% of the human population is EBV-infected, EBV-driven pathologies including B cell lymphomas are limited by a potent T cell immune response. Here, we present a mouse model for acute EBV infection through conditional expression of two key EBV proteins, LMP1 and LMP2A. This model reproduces EBV-driven B cell expansion, T cell-mediated immune surveillance of EBV-infected B cells and fatal lymphoproliferative disease when the T cell response is compromised like in immunosuppressed or genetically impaired patients. It thus allows one to study EBV–host interaction functionally and from a new angle, and should help to develop new therapies for EBV-driven hematological diseases.

\body

Introduction

Epstein-Barr Virus (EBV) is a γ -herpes virus that infects human B cells and growth-transforms them *in vitro*. Infection is usually asymptomatic, but can lead to infectious mononucleosis (IM) in teenagers and adults (1). EBV drives infected B cells into proliferation, but the symptoms of IM, mainly fever, lymphadenopathy and splenomegaly, are believed to result from the subsequent activation and massive proliferation of EBV-reactive T cells (2). After the acute phase of infection, EBV persists in a small subset of memory B cells throughout life and is kept in check by memory T cells (2–4). While an EBV infection is harmless to most people, immunocompromised individuals can develop severe complications. Genetic defects that lead to impaired T cell function predispose to EBV-driven lymphoproliferative diseases, such as familial hemophagocytic lymphohistiocytosis (FHL) (5, 6). FHL presents in infants and is characterized by persistent fever, hemophagocytosis and cytokine storms. These symptoms are attributed to proliferation and cytokine production by macrophages and T cells (5–7). About one third of FHL cases are caused by mutations in the *PRF1* gene encoding perforin (8). EBV is also highly associated with HIV-related and post-transplantation lymphomas (PTL), which are usually derived from germinal center (GC) B cells. Most likely EBV is the causative agent for these lymphomas, transforming GC B cells when T cell immunosurveillance is impeded owing to HIV infection or immunosuppressive therapy after organ transplantation (1, 9, 10).

The activation and proliferation of EBV-infected B cells is induced by virus-encoded proteins, with latent membrane protein 1 (LMP1) and LMP2A playing a prominent role. These proteins mimic signaling from the CD40 receptor and from the B cell receptor (BCR), respectively (11–17). LMP1 activates proliferation and survival, for example via the NF- κ B and JNK pathways (18). LMP2A activates PI3K signaling via Lyn and Syk protein tyrosine kinases (19). LMP1 is essential for the growth-transformation potential of EBV *in vitro* (18, 20).

EBV infection cannot be directly studied in mice because the virus is endemic to humans. In an attempt to overcome this problem, we and others have expressed LMP1 or LMP2A in mouse B cells (3, 4, 6, 20–23). Transgenic mice that express LMP1 in B cells develop lymphomas beginning at 12 months of age (16). Expression of LMP2A instead of the BCR allows mouse B cells to circumvent regular B cell development and to form relatively normal B cell compartments (13). Conditional expression of LMP2A in mouse GC B cells disturbs affinity maturation and leads to lupus-like symptoms in aged mice (23). More recent own studies, in which LMP1 was conditionally expressed in mouse B cells, showed that this single EBV protein is sufficient to provide B cells with the ability to elicit tight T cell immunosurveillance and, in the absence of immunosurveillance, to proliferate and eventually give rise to B cell lymphomas (21, 22). While earlier *in vivo* studies have offered insights into the role of LMP1 as an oncogene and of LMP2A as a BCR surrogate, little attention has been paid to the immune response against LMP-expressing B cells. As LMP1 and LMP2A are typically expressed together (2), we have now generated a mouse model of conditional LMP1/2A co-expression, where LMP expression is induced in a timed manner and only in a fraction of B cells, like in acute EBV infection in humans.

Results

Combined expression of LMP1 and LMP2A in early B cell development is lethal.

We created a *Rosa26* allele allowing expression of LMP2A together with a GFP reporter upon Cre/loxP-mediated excision of a transcriptional/translational STOP cassette (LMP2A^{fSTOP}). LMP2A^{fSTOP} mice were then crossed to CD19-Cre; LMP1^{fSTOP} mice, which express LMP1 and a human CD2 (hCD2) reporter from the *Rosa26* locus and a Cre recombinase that activates transgenes in late pro-B cells (21, 22). CD19-Cre; LMP1/LMP2A^{fSTOP} mice died on day 4 or 5 after birth, with 100 % penetrance. Neonatal death was not observed in mice expressing LMP1 or LMP2A alone (Fig. 1A), the former in agreement with our previous work (21, 22). CD19-Cre; LMP1/LMP2A^{fSTOP} newborns showed strongly enlarged spleens and livers and severe infiltration of blastic B cells (FSC^{high}CD19⁺GFP⁺Fas⁺) into organs such as spleen, liver, and lung (Fig. 1 A and B). Because most of the expanded B cells did not express surface IgM (Fig. S1A) but were CD19⁺, they were likely derived from B cell progenitors, with LMP2A expression possibly providing a component of BCR signaling (14). Because we previously reported that T and NK cells play an important role in the immune surveillance of LMP1 expressing B cells (21), we evaluated cell numbers and activation status (CD69 expression) of T and NK cells in spleens of day 3 newborns. Although T cells made up minor fractions compared to B and NK cells, LMP1 expressing mice showed increased numbers and activation of CD4, CD8, and $\gamma\delta$ T cells (Fig. 1C). Activation of T and NK cells was also observed in mice co-expressing LMP1 and LMP2A in B cells (Fig. 1D), but these animals exhibited a large expansion of LMP1/2A-expressing B cells concomitant with reduced T and NK cell expansion, and eventually succumbed to organ failure (Fig. 1 A and C). Rag2^{-/-} γ C^{-/-} recipient mice reconstituted with bone marrow hematopoietic stem cells (HSCs) from 3 day old CD19-Cre; LMP1/LMP2A^{fSTOP} mice died at 23-32 days after HSCs transplantation (Fig. S1B). Those terminally ill mice had severe hyperplasia of LMP1⁺LMP2A⁺ B cells in bone marrow and spleen, even though T and NK cells were activated (Fig. S1C and D). Death of recipients was not observed when CD19-Cre; LMP1^{fSTOP} or CD19-Cre; LMP2A^{fSTOP} HSCs were used

for reconstitution (Fig. S1B). These data indicate that combined expression of LMP1 and LMP2A in B cells early in life is lethal.

Expression of LMP1 and LMP2A in a small number of mature B cells as a model for acute EBV infection.

In order to model EBV infection more faithfully by restricting it to just a few initially infected naïve B cells, we crossed LMP1^{fSTOP} and LMP2A^{fSTOP} animals with CD19-Cre^{ERT2} animals (22). Tamoxifen treatment of these mice led to expression of LMP1 and LMP2A in a small population of splenic B cells (~ 2 - 5 %), as seen in reporter control animals crossed to CD19-Cre^{ERT2} (Fig. 2A). While the number of reporter⁺ B cells in these latter animals was stable over time, expression of LMP1, alone or together with LMP2A, led to strong cellular expansion of B cells, reaching its maximum on day 6 to 7 after tamoxifen treatment (Fig. 2B). The surface phenotype of these cells (CD19⁺CD38^{high}IgD^{high}) suggests that they originate from naïve follicular B cells (Fig. S2A). This was followed by a strong expansion of T cells, mainly of the CD8 subset, accompanied by a dramatic reduction of reporter⁺ B cells. The strong lymphoproliferation led to splenomegaly and liver infiltration of T and B cells between day 5 and 8. However, reporter⁺ B cells were no longer observed from day 10 on (Fig. 2B and C).

The expanding T cells developed the phenotype of effector/memory T cells at around day 6 after tamoxifen treatment, as seen by loss of CD62L and gain of CD44 and PD-1 (Fig. 2D, Fig. S2B). Both CD4 and CD8 T cells showed classical pro-inflammatory TNF α and IFN γ expression (Fig. S2C). At later timepoints, more than half of the CD8 T cells of CD19-Cre^{ERT2}; LMP1/LMP2A^{fSTOP} mice were still high in CD44 surface expression, an established marker for memory T cells (Fig. 2D), suggesting the formation of immunological memory.

To investigate whether T cells from tamoxifen-treated animals directly kill LMP1/LMP2A-expressing B cells or interfere with B cell expansion indirectly, we performed killing assays with activated CD8 T cells from CD19-Cre^{ERT2}; LMP1^{fSTOP} mice 8 days after tamoxifen treatment. Activated T cells induced

cytolysis in transformed LMP1-expressing cells as well as primary LMP1 blasts, but not in syngeneic B-lymphoma cells from a Burkitt mouse model (24) or MHC-I-deficient transformed LMP1⁺ B cells (Fig. 3A). Similarly, LMP1^{fSTOP} B cells, in which expression of LMP1 was induced *in vitro* by TAT-Cre treatment, were killed by activated T cells from these mice, but not LMP1^{fSTOP} B cells activated by anti-CD40 stimulation (Fig. S2D). None of these targets were killed by T cells isolated from CD19-Cre^{ERT2}; hCD2^{fSTOP} mice 8 days after tamoxifen treatment. These results indicate that the activated CD8 T cells kill LMP-driven B cell blasts in an antigen-specific, MHC-restricted manner, in line with our earlier data on T cell surveillance of LMP1-induced B cell lymphomas in the mouse (21) and data from the human (25).

To test whether the T cells are indeed controlling LMP1/LMP2A expressing B cell outgrowth in our IM model, we performed antibody-mediated T cell depletion in CD19-Cre^{ERT2}; LMP1/LMP2A^{fSTOP} animals shortly before tamoxifen treatment. Animals that were not T cell-depleted showed large numbers of T cells, while reporter⁺ B cells were absent on day 9 after tamoxifen treatment. Conversely, animals that were treated with T cell depleting antibodies showed strong expansion of reporter⁺ B cells in the spleen (Fig. 3B). Of note, in the course of this experiment some T cell-depleted animals reached termination criteria, likely due to overwhelming expansion of reporter⁺ B cells.

Modeling fatal EBV infection.

While the healthy human immune system is able to control EBV-infection, a number of primary immunodeficiencies predispose patients to fatal EBV-associated hematological diseases (5, 6). Among those are inactivating mutations of perforin, a protein that is required for Granzyme-mediated T cell killing. Because we observed that direct CD8 T cell-mediated killing is involved in the control of LMP1/LMP2A-expressing B cells in our mouse model, we crossed CD19-Cre^{ERT2}; LMP1^{fSTOP} and CD19-Cre^{ERT2}; LMP1/LMP2A^{fSTOP} animals with perforin-deficient animals. When these mice were treated with tamoxifen, more than 75 % of animals reached termination criteria on day 6 after tamoxifen treatment (Fig. 3 C), with pronounced spleen and liver infiltration with reporter⁺

B cells compared to perforin-sufficient animals (Fig. S2E). Strong activation of T cells could be observed in both perforin-sufficient and -deficient animals (Fig. S2F). Thus, the present mouse model of acute EBV infection opens the way to a functional analysis of at least one of the EBV-related human immunodeficiencies.

Expression of LMP1 and LMP2A in GC B cells leads to fatal B cell expansion upon immunosuppressive treatment.

We then studied the function of LMP1 and LMP2A in GC B cells, as these proteins are frequently co-expressed in GC-derived EBV⁺ lymphomas. We used C γ 1-Cre, which is active in GC B cells (26), to drive expression of LMP1 and LMP2A, either alone or in combination. 10 days after immunization with the hapten 4-hydroxy-3-nitro-phenylacetyl coupled to chicken gamma globulin (NP-CGG) we analyzed the frequencies of GC B cells (CD19⁺Fas^{high}CD38^{low}) in the spleen (Fig. 4A). Control mice expressing only the reporter showed a clear GC population, while in C γ 1-Cre; LMP1^{fSTOP} mice the frequency of GC B cells was markedly reduced. This reduction was even more pronounced when LMP2A was co-expressed. The total number of reporter⁺ cells was similarly reduced (Fig. 4C). Expression of LMP2A alone had no significant effect (Fig. 4 B and C).

Interestingly, the few reporter⁺ cells found in C γ 1-Cre; LMP1^{fSTOP} mice were able to proliferate when they were isolated and cultured *in vitro* and this proliferation was stronger when LMP2A was co-expressed (Fig. S3A and B). To test whether LMP expressing GC B cells are under T cell immunosurveillance, we treated mice expressing LMP1 and/or LMP2A in GC B cells with a T cell-depleting antibody cocktail starting on day 10 after immunization. This led to massive expansion of GC B cells co-expressing LMP1 and LMP2A, but not of GC B cells expressing LMP1 or LMP2A alone (Fig. 4 B and C). This expansion was ultimately fatal (Fig. 4D) and was associated with enlarged spleens (Fig. S3C), where GCs were histologically undetectable (Fig. S3D). Analysis of IgH VH gene usage showed that the expanding B cell population was polyclonal in nature (Fig. S3E). The surface marker profile of the expanding LMP1/LMP2A expressing cells resembled that of GC B cells (Fas^{high}CD38^{low}IgD⁻), but the cells remained IgM⁺ (Fig. S3F). GC B cells are in part defined by somatic mutations in their rearranged

immunoglobulin variable region genes. Mutation analysis (27–29) of the IgH JH4 intron showed that the expanding LMP1/LMP2A expressing cells had only few mutations compared to normal GC B cells (Fig. 4E). This suggests that these cells were derived from pre- and early GC B cells, and that the LMPs halt somatic mutation once they are expressed. The cells up-regulated surface molecules important for the interaction with T cells, such as CD80, CD86, ICAM-1, and the activation marker CD69 (Fig. S3G). Treatment of the animals with T cell depleting antibodies reduced the total number of splenic T cells by 90% except for mice co-expressing LMP1 and LMP2A in GC B cells, where concomitantly with the expansion of B cells the T cell numbers increased again (Fig. 4C and S4A). This is likely due to the immunogenicity of expanding LMP1/LMP2A expressing GC B cells, activating and expanding the few T cells that remain after depletion. Western blot analysis confirmed that in our mouse model LMP1 expression leads to phosphorylation of Erk and Jnk, while LMP2A expression leads to phosphorylation of Akt, and that all of these factors are strongly phosphorylated in LMP1/LMP2A co-expressing cells (Fig. S4B). Phosphorylation of Akt is mediated through PI3K activation, an important signaling factor downstream of BCR signaling. To test whether PI3K activation alone is sufficient to explain the function of LMP2A in our model, we replaced LMP2A by P110*, a constitutively active form of PI3K (30). Indeed, mice that co-express LMP1 and P110* in GC B cells exhibited a similar B cell expansion as mice that co-express LMP1 and LMP2A when immunized and subsequently treated with T cell-depleting antibodies (Fig. 4F). The expansion of T cells that remain after depletion can also be observed in these mice, indicating that LMP1/ P110* co-expressing B cells are as immunogenic as LMP1/LMP2A co-expressing B cells (Fig. S4C).

Discussion

Previous genetic models have shown that LMP1 expression in early B cells is sufficient to model some key features of EBV infection in mice, namely the immunogenicity of LMP1-expressing B cells (21, 22) and their potential to form tumors (16, 21), despite the fact that EBV is endemic to humans. The previously described T cell immunosurveillance of LMP1-expressing mouse B cells stands in contrast to the widely held belief that the human immune system has evolved to specifically prevent the expansion of EBV-infected B cells and that this is accomplished by a T cell repertoire that recognizes a wide range of peptide epitopes mainly derived from EBV nuclear antigens (EBNAs) and lytic antigens (31). Based on the earlier mouse studies and the present findings, one may speculate that the virus has evolved to be recognized by the immune system, likely because life long latent infection creates an advantage over fatal infection. Apparently, LMP1 plays a critical role in this process.

The present study was designed to determine the effects of combined LMP2A and LMP1 expression in mouse B cells and to better mimic viral infection by timed and restricted expression of the LMPs. LMP1/LMP2A co-expression under the control of CD19-Cre in early B cells was lethal, as opposed to LMP1 or LMP2A single-expression (Fig. 1). We therefore induced expression of LMP1 and LMP2A using the CD19-Cre^{ERT2} allele and tamoxifen such that expression occurred in only a small fraction of naïve B cells in adult mice. This system faithfully recapitulated the initial expansion of EBV-infected (LMP1 and LMP2A co-expressing) B cell blasts in human IM, the subsequent activation and expansion of T cells and the clearance of the B cell blasts (Fig. 2). Immunosuppressive treatment by T cell depletion led to uncontrolled expansion of B cells co-expressing LMP1 and LMP2A (Fig. 3). We also showed that this system can be used to model at least one form of FHL, by crossing the mice to a *Prf1*-deficient background. While *Prf1*-proficient T cells were able to control LMP1- and LMP2A- expressing B cell blasts, *Prf1*-deficient T cells failed to do so (Fig. 3). Further work will show whether other genetic deficiencies that are responsible for primary immunodeficiencies, such as SLAM-associated protein (*Sh2d1a/Sap*)

and interleukin-2-inducible T-cell kinase (*Itk*) deficiency (5), will lead to similar phenotypes.

EBV is associated with B cell malignancies like Burkitt-, Hodgkin-, AIDS-associated, and post-transplant lymphoma, all of which are usually derived from GC B cells. LMP1 and LMP2A are suspected to drive transformation of GC B cells, LMP1 as a growth-promoting oncogene and LMP2A as a BCR-surrogate that rescues EBV-infected GC B cells from apoptosis once they have acquired “crippling” somatic mutations that lead to loss of BCR expression (9, 10). When we expressed LMP1, either alone or together with LMP2A, under the control of $\text{C}\gamma 1\text{-Cre}$ in pre- and early GC B cells, reporter⁺ B cells were under efficient T cell immunosurveillance. Depletion of T cells beginning on day 10 after immunization led to fatal expansion of LMP1/LMP2A co-expressing GC B cells. Notably, however, this was not the case for LMP1 or LMP2A single-expressing GC cells (Fig. 4). LMP2A might therefore play a role in GC B cell transformation that goes beyond the well-described rescue of GC B cells that have acquired “crippling” somatic mutations (9) (Fig. 4). By replacing LMP2A with an active form of PI3K, we showed that activation of PI3K is likely the major mechanism by which LMP2A co-expression with LMP1 causes a phenotype that so dramatically differs from LMP1 single-expression (Fig. 4). In an earlier study by Longnecker and colleagues (32), LMP1 and LMP2A were co-expressed in the entire B cell compartment in mice. Here LMP2A appeared to negatively modulate the function of LMP1, rescuing the loss of GC B cells caused by LMP1 expression. A clear difference with respect to our previous and present work is the presence of large numbers of LMP expressing cells in the mice analyzed by Vrazo et al., suggesting that the levels of LMP1 expression were insufficient to induce T cell immune surveillance as it is seen in the present mouse model and in human EBV infection. Indeed, there is evidence that LMP2A augments LMP1 signaling in human EBV infected cells (33).

$\text{C}\gamma 1\text{-Cre}$ -driven expression of LMP1 and LMP2A in mouse GC B cells should help to clarify the question as to whether these two factors are sufficient for the transformation of GC B cells, resulting in the development of GC-derived

lymphomas. However, the rapid and fatal polyclonal expansion of LMP-expressing GC cells makes it impossible to study lymphomagenesis in our current model. C γ 1-Cre lacks the advantage of CD19-Cre^{ERT2} to drive transgene expression in a timed manner in a small fraction of cells. It will therefore be interesting to drive LMP1/LMP2A expression by a novel C γ 1-Cre^{ERT2} allele which we have recently generated.

Taken together, co-expression of LMP1 and LMP2A in either follicular or GC B cells of the mouse allows one to generate pre-clinical models for a range of EBV-associated pathologies, from FHL to AIDS-associated and post-transplant lymphomas, opening the way to the development of therapeutic approaches such as gene correction in the case of inherited EBV related immunoproliferative syndromes.

Materials and Methods

Additional information is provided in *Supplementary Materials and Methods*.

Mice. Previously described CD19-Cre (34), CD19-Cre^{ERT2} (22), and C γ 1-Cre (26) mice were generated by targeting 129P2-derived embryonic stem (ES) cells and backcrossing to C57BL/6. Previously described LMP1^{flSTOP} (21), hCD2^{flSTOP} (35), Prf^{-/-} (36), and P110^{*flSTOP} (30) mice were generated by targeting C57BL/6-derived ES cells. Rag2^{-/-} γ C^{-/-} mice (37) were from Taconic. LMP2A^{flSTOP} mice were generated by cloning the LMP2A coding sequence derived from the EBV B95-8 strain in-between a loxP-flanked STOP cassette and an IRES-GFP reporter and targeting into the Rosa26 locus of C57BL/6-derived ES cells. To activate Cre^{ERT2}, 4 mg tamoxifen (Sigma), dissolved in sunflower oil (Sigma), was fed by oral gavage. For T-cell-dependent immunization, mice were injected intraperitoneally with 100 μ g NP-CGG (Biosearch) precipitated in alum (Sigma). For antibody-mediated T cell depletion, mice were injected intraperitoneally with a mix of anti-CD4 (YTS 191.1.2), anti-CD8 (YTS 169.4.2.1), and anti-Thy-1 (YTS 154.7.7.10) antibodies in PBS, 400 μ g each. Animals were maintained in specific pathogen-free conditions and handled according to protocols approved by the LaGeSo Berlin or by the Harvard University Institutional Animal Care and Use Committee and by the Immune Disease Institute.

Acknowledgments

We thank Dr. S. Cobbold for the anti-CD4, -CD8, and -Thy1 hybridomas, Dr. T. Blankenstein for providing Prf^{-/-} mice, Dr. A. Franklin for critical reading of the manuscript, and Dr. S. Sander for somatic mutation analysis; We are grateful to A. Hesseling, M. Bamberg, C. Grosse, K. Petsch, J. Pempe, and J. Woehlecke for technical assistance. This work was supported by grants from the US National Institutes of Health and the European Research Council (Advanced Grant 268921) to K.R.. T.Y. was supported by a JSPS Postdoctoral Fellowship for Research Abroad and by the Astellas Foundation for Research on Metabolic Disorders. T.S. is supported by a PCCC grant. S.K. is a CNRS researcher.

Author contributions

T.Wi., T.We., T.S., and T.Y. performed experiments and analyzed data; S.K. generated LMP2A^{flSTOP} mice; T.Wi., T.We., T.S., K.R., and T.Y. designed research and wrote the paper.

References

1. Kutok JL, Wang F (2006) Spectrum of Epstein-Barr virus-associated diseases. *Annu Rev Pathol* 1:375–404.
2. Cohen JI (2000) Epstein-Barr virus infection. *N Engl J Med* 343(7):481–92.
3. Babcock GJ, Decker LL, Volk M, Thorley-Lawson D a (1998) EBV persistence in memory B cells in vivo. *Immunity* 9(3):395–404.
4. Hislop AD, Taylor GS, Sauce D, Rickinson AB (2007) Cellular responses to viral infection in humans: lessons from Epstein-Barr virus. *Annu Rev Immunol* 25:587–617.
5. Parvaneh N, Filipovich AH, Borkhardt A (2013) Primary immunodeficiencies predisposed to Epstein-Barr virus-driven haematological diseases. *Br J Haematol* 162(5):573–86.
6. Sieni E, et al. (2014) Familial hemophagocytic lymphohistiocytosis: when rare diseases shed light on immune system functioning. *Front Immunol* 5:167.
7. Stepp SE, et al. (1999) Perforin gene defects in familial hemophagocytic lymphohistiocytosis. *Science* 286(5446):1957–9.
8. Zur Stadt U, et al. (2006) Mutation spectrum in children with primary hemophagocytic lymphohistiocytosis: molecular and functional analyses of PRF1, UNC13D, STX11, and RAB27A. *Hum Mutat* 27(1):62–8.
9. Mancao C, Altmann M, Jungnickel B, Hammerschmidt W (2005) Rescue of crippled germinal center B cells from apoptosis by Epstein-Barr virus. *Blood* 106(13):4339–44.
10. Küppers R (2003) B cells under influence: transformation of B cells by Epstein-Barr virus. *Nat Rev Immunol* 3(10):801–12.
11. Mancao C, Hammerschmidt W (2007) Epstein-Barr virus latent membrane protein 2A is a B-cell receptor mimic and essential for B-cell survival. *Blood* 110(10):3715–21.
12. Young LS, Rickinson AB (2004) Epstein-Barr virus: 40 years on. *Nat Rev Cancer* 4(10):757–68.
13. Caldwell RG, Wilson JB, Anderson SJ, Longnecker R (1998) Epstein-Barr Virus LMP2A Drives B Cell Development and Survival in the Absence of Normal B Cell Receptor Signals. *Immunity* 9(3):405–411.

14. Casola S, et al. (2004) B cell receptor signal strength determines B cell fate. *Nat Immunol* 5:317–327.
15. Wang D, Liebowitz D, Kieff E (1985) An EBV membrane protein expressed in immortalized lymphocytes transforms established rodent cells. *Cell* 43(3 Pt 2):831–40.
16. Kulwichit W, et al. (1998) Expression of the Epstein-Barr virus latent membrane protein 1 induces B cell lymphoma in transgenic mice. *Proc Natl Acad Sci U S A* 95(20):11963–8.
17. Mainou BA, Everly DN, Raab-Traub N (2005) Epstein-Barr virus latent membrane protein 1 CTAR1 mediates rodent and human fibroblast transformation through activation of PI3K. *Oncogene* 24(46):6917–24.
18. Kilger E, Kieser a, Baumann M, Hammerschmidt W (1998) Epstein-Barr virus-mediated B-cell proliferation is dependent upon latent membrane protein 1, which simulates an activated CD40 receptor. *EMBO J* 17(6):1700–9.
19. Swart R, Ruf IK, Sample J, Longnecker R (2000) Latent membrane protein 2A-mediated effects on the phosphatidylinositol 3-Kinase/Akt pathway. *J Virol* 74(22):10838–45.
20. Kaye KM, Izumi KM, Kieff E (1993) Epstein-Barr virus latent membrane protein 1 is essential for B-lymphocyte growth transformation. *Proc Natl Acad Sci U S A* 90(19):9150–4.
21. Zhang B, et al. (2012) Immune surveillance and therapy of lymphomas driven by Epstein-Barr virus protein LMP1 in a mouse model. *Cell* 148(4):739–51.
22. Yasuda T, et al. (2013) Studying Epstein-Barr virus pathologies and immune surveillance by reconstructing EBV infection in mice. *Cold Spring Harb Symp Quant Biol* 78(1):259–263.
23. Minamitani T, et al. (2015) Evasion of affinity-based selection in germinal centers by Epstein-Barr virus LMP2A. *Proc Natl Acad Sci U S A* 112(37):11612–7.
24. Sander S, et al. (2012) Synergy between PI3K Signaling and MYC in Burkitt Lymphomagenesis. *Cancer Cell* 22(2):167–179.
25. Maini MK, Gudgeon N, Wedderburn LR, Rickinson AB, Beverley PC (2000)

- Clonal expansions in acute EBV infection are detectable in the CD8 and not the CD4 subset and persist with a variable CD45 phenotype. *J Immunol* 165(10):5729–37.
26. Casola S, et al. (2006) Tracking germinal center B cells expressing germline immunoglobulin gamma1 transcripts by conditional gene targeting. *Proc Natl Acad Sci U S A* 103(19):7396–401.
 27. Kaji T, et al. (2012) Distinct cellular pathways select germline-encoded and somatically mutated antibodies into immunological memory. *J Exp Med* 209(11):2079–97.
 28. Jolly CJ, Klix N, Neuberger MS (1997) Rapid methods for the analysis of immunoglobulin gene hypermutation: application to transgenic and gene targeted mice. *Nucleic Acids Res* 25(10):1913–9.
 29. Xue K, Rada C, Neuberger MS (2006) The in vivo pattern of AID targeting to immunoglobulin switch regions deduced from mutation spectra in *msh2*^{-/-} *ung*^{-/-} mice. *J Exp Med* 203(9):2085–94.
 30. Srinivasan L, et al. (2009) PI3 kinase signals BCR-dependent mature B cell survival. *Cell* 139(3):573–586.
 31. Taylor GS, Long HM, Brooks JM, Rickinson AB, Hislop AD (2015) The immunology of Epstein-Barr virus-induced disease. *Annu Rev Immunol* 33:787–821.
 32. Vrazo AC, Chauchard M, Raab-Traub N, Longnecker R (2012) Epstein-Barr virus LMP2A reduces hyperactivation induced by LMP1 to restore normal B cell phenotype in transgenic mice. *PLoS Pathog* 8(4):e1002662.
 33. Dawson CW, George JH, Blake SMS, Longnecker R, Young LS (2001) The Epstein-Barr Virus Encoded Latent Membrane Protein 2A Augments Signaling from Latent Membrane Protein 1. *Virology* 289(2):192–207.
 34. Rickert RC, Roes J, Rajewsky K (1997) B lymphocyte-specific, Cre-mediated mutagenesis in mice. *Nucleic Acids Res* 25(6):1317–1318.
 35. Calado DP, et al. (2012) The cell-cycle regulator c-Myc is essential for the formation and maintenance of germinal centers. *Nat Immunol* 13(11):1092–1100.
 36. Kägi D, et al. (1994) Cytotoxicity mediated by T cells and natural killer cells is greatly impaired in perforin-deficient mice. *Nature* 369:31–37.

37. Garcia S, DiSanto J, Stockinger B (1999) Following the development of a CD4 T cell response in vivo: from activation to memory formation. *Immunity* 11(2):163–71.

Figure legends

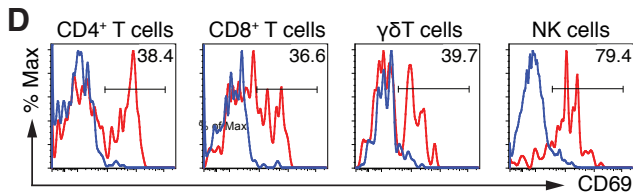
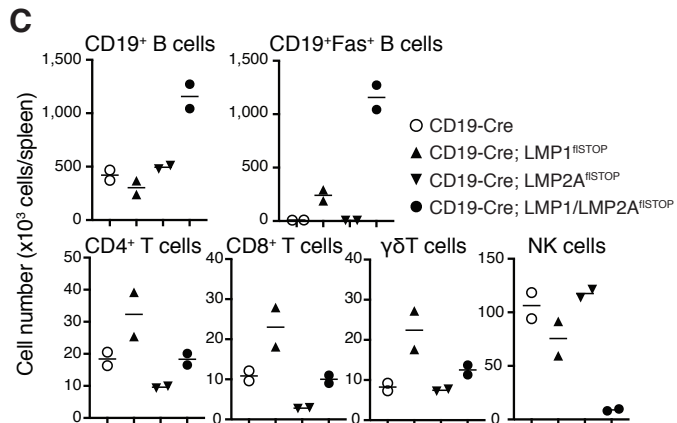
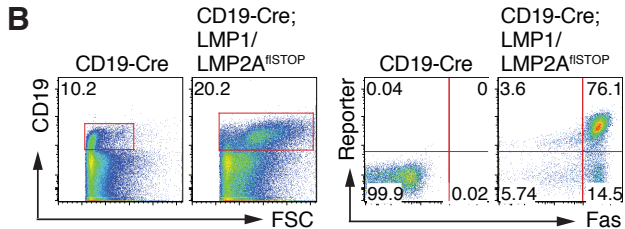
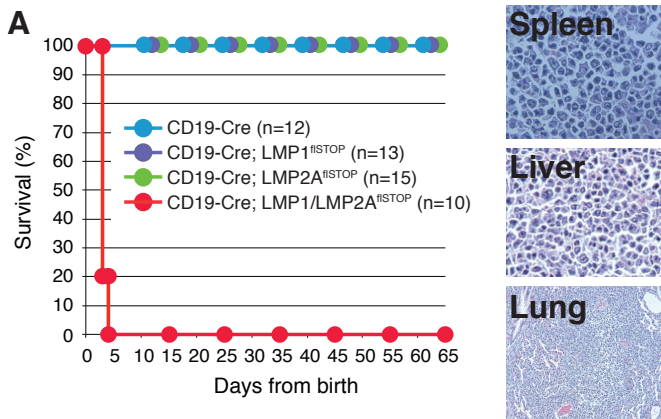
Figure 1. Combined expression of LMP1 and LMP2A in early B cell development leads to neonatal death. **(A)** Survival of mice with the indicated genotype and representative HE staining of spleen (400x), liver (200x) and lung (100x) of CD19-Cre; LMP1/LMP2A^{fSTOP} animals. **(B)** FACS analysis of spleen cells from CD19-Cre and CD19-Cre; LMP1/LMP2A^{fSTOP} animals. Fas expression is a surrogate marker for LMP1 expression in B cells. Reporter; GFP reporter for LMP2A. **(C)** Cell numbers of indicated cell types in spleens of P3 mice. Each dot indicates one mouse. Results are representative for two independent analyses. **(D)** FACS analysis of the activation status represented by CD69 expression of splenic T and NK cells. Blue: CD19-Cre, Red: CD19-Cre; LMP1/LMP2A^{fSTOP}. **(B and D)** Representative data for more than four individual mice.

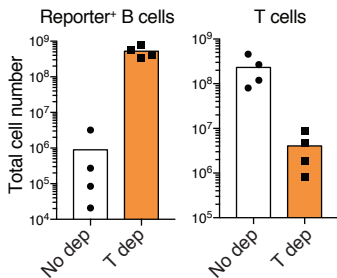
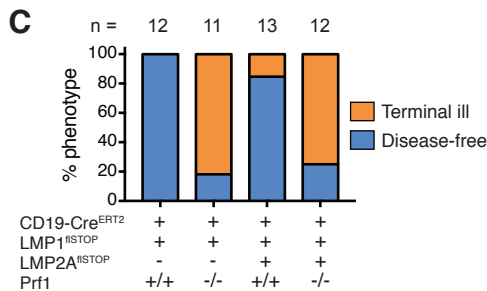
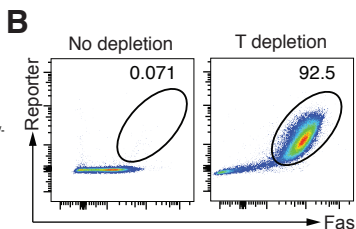
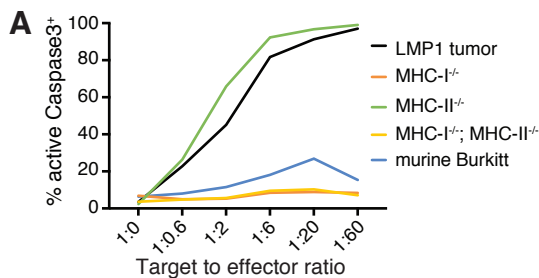
Figure 2. A model for acute EBV infection. **(A)** Representative FACS plots of splenocytes from mice of indicated genotypes, gated on all live cells. **(B)** Spleen weight and cell number of indicated cell types in spleens at indicated time points after tamoxifen treatment. Error bars show standard deviation and dots indicate single animals, at least 3 per graph. **(C)** Representative spleens and livers from CD19-Cre^{ERT2}; LMP1/LMP2A^{fSTOP} mice at indicated time points after tamoxifen treatment. Liver lymphocyte infiltrations are shown by arrows. Representative of more than four independent experiments. **(D)** Representative FACS plots of splenic CD8 T cells from CD19-Cre^{ERT2}; LMP1/LMP2A^{fSTOP} mice for CD44 and CD62L surface expression.

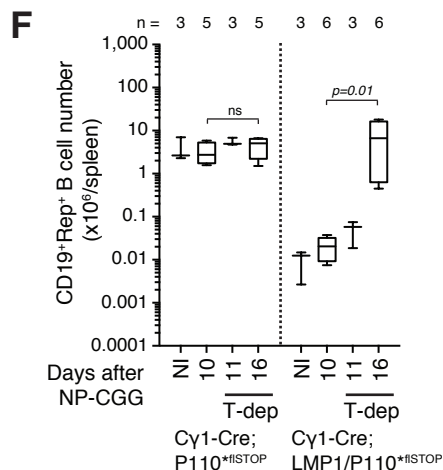
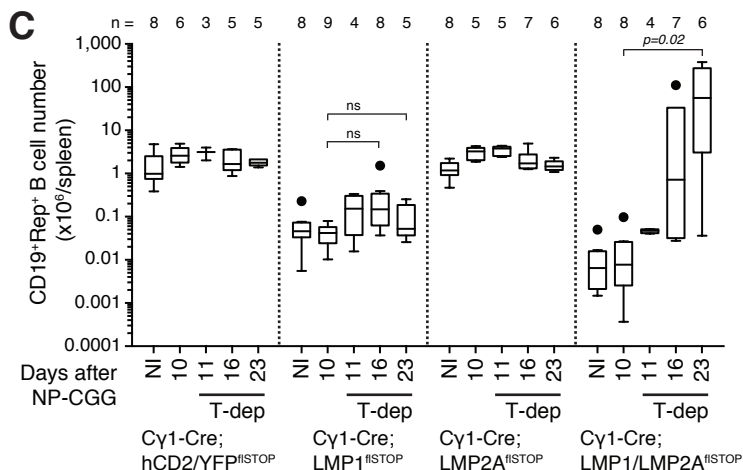
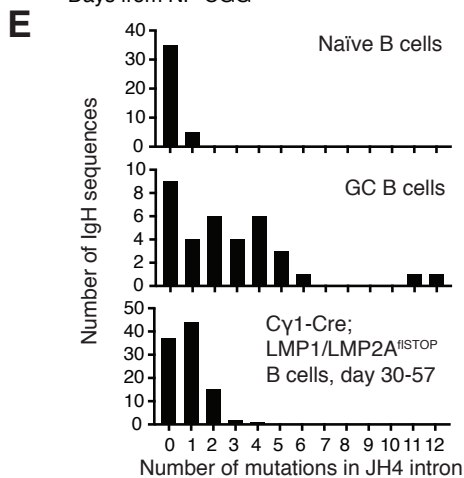
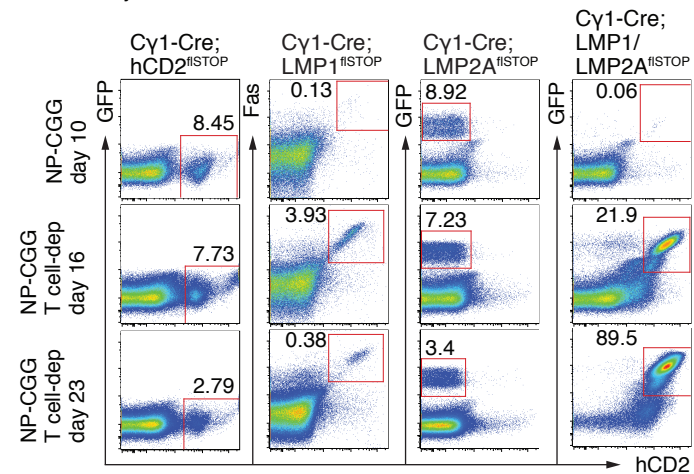
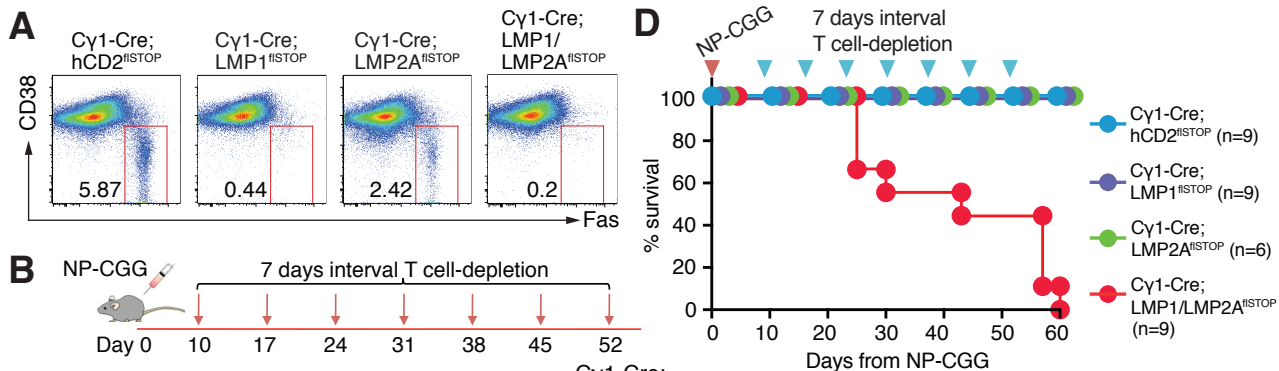
Figure 3. A mouse model for fatal infectious mononucleosis. **(A)** Killing assay of transformed LMP1- and LMP2A-expressing B cells co-cultured with activated T cells isolated from CD19-Cre^{ERT2}; LMP1^{fSTOP} mice on day 8 after tamoxifen treatment. Representative for 3 independent experiments. **(B)** Representative FACS plots of splenocytes and quantitative analysis of reporter⁺ B or TCR β ⁺ T cell numbers from CD19-Cre^{ERT2}; LMP1/LMP2A^{fSTOP} mice on day 9 after tamoxifen either with or without T cell depletion 3 and 5 days before tamoxifen. Dots indicate single animals. **(C)** Percentage of animals with the

indicated genotypes reaching termination criteria on day 6 after tamoxifen treatment. Numbers of mice are indicated above the graphs.

Figure 4. Conditional expression of LMP1 and LMP2A in GC B cells leads to fatal B cell expansion upon immunosuppressive treatment. **(A)** Indicated mice were immunized with NP-CGG and spleen cells were analyzed on day 10. Percentages of GC B cells within CD19⁺ B cells are shown. **(B)** Same mice as in A were treated with T cell-depleting antibodies in a 7 day interval starting on day 10 after immunization. Percentages of reporter⁺ cells within CD19⁺ B cells are shown. **(A and B)** Representative data of more than four independent experiments. **(C)** Quantification of reporter⁺ splenic B cells in the experiments shown in A and B. **(D)** Survival curve of mice from the experiment shown in B. Representative data of two independent experiments. **(E)** Somatic mutation analysis of expanding B cells sorted from sick C γ 1-Cre; LMP1/LMP2A^{fSTOP} animals that were treated as in B. As control, naïve and GC B cells isolated from spleens of C57BL/6 mice on day 10 after SRBC immunization were used. Frequency distribution of somatic mutations per IgH JH4 intron and absolute numbers of analyzed sequences are shown. **(F)** Number of reporter⁺ splenic B cells in mice of indicated genotypes after NP-CGG immunization, followed by T cell depletion on day 10. NI; no immunization. **(C and F)** Data are representative for three independent experiments.







Supporting Information

Wirtz et al. 2016

Supplemental figure legends

Figure S1. Combined expression of LMP1 and LMP2A in early B cell development is lethal. **(A)** IgM expression levels and % of IgM⁺ in day 3 newborn splenic B cells. Blue: CD19⁺ cells from CD19-Cre mouse, Red: CD19⁺Reporter⁺ cells from CD19-Cre; LMP1/LMP2A^{fSTOP} mouse. **(B)** Survival of Rag2^{-/-}γC^{-/-} recipient mice reconstituted with bone marrow HSCs from day 3 newborns of indicated genotypes. **(C)** FACS analysis of recipient bone marrow (BM) and spleen (SP) cells from CD19cre; LMP1/LMP2A^{fSTOP} HSC reconstitution. Fas expression is a surrogate marker for LMP1 expression and GFP represents LMP2A expression. **(D)** FACS analysis of the activation status represented by CD69 expression on splenic T and NK cells. Blue: CD19-Cre HSC reconstitution, Red: CD19cre; LMP1/LMP2A^{fSTOP} HSC reconstitution. **(C and D)** Representative data of more than four individual mice.

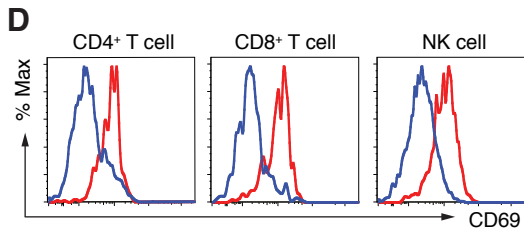
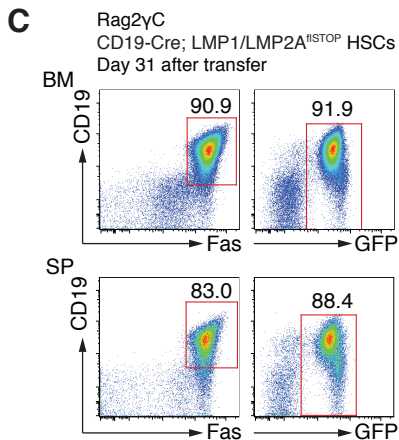
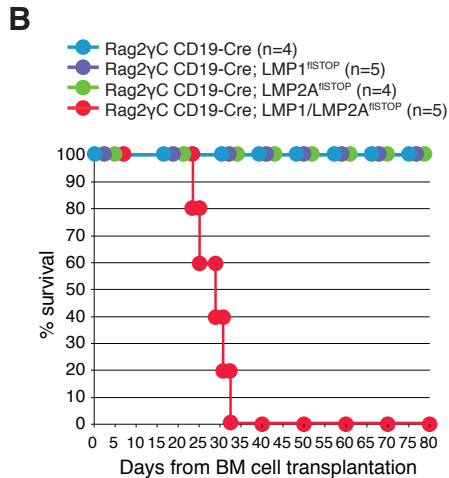
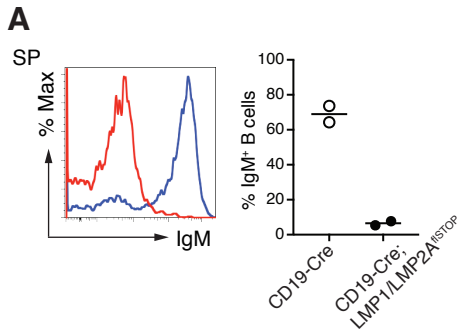
Figure S2. Activation status, cytokine expression and cytolytic activity of T cells from acute EBV infection mouse models. **(A)** Representative FACS analysis of surface marker expression on day 6 after tamoxifen treatment. Reporter⁺ splenic B cells are gated for the analysis. **(B)** Representative FACS analysis of PD-1 expression in splenic T cells from mice of indicated genotypes at indicated time points after tamoxifen treatment. Tumor; LMP1 tumor cell line. LMP1 B; LMP1-expressing blastic B cells. CD40 B; CD40-stimulated blastic B cells. **(C)** Representative FACS analysis of splenic CD4 and CD8 T cells from mice of indicated genotypes on day 7 after tamoxifen treatment. Cells were stimulated for 6 hrs with PMA and ionomycin and stained intracellularly. **(D)** Representative killing assay of LMP1-expressing tumor cells, primary LMP1-expressing or anti-CD40-stimulated B cells, co-cultured with T cells isolated from CD19cre^{ERT2}; LMP1^{fSTOP} or CD19cre^{ERT2}; hCD2^{fSTOP} mice on day 8 after tamoxifen treatment. **(E)** Representative FACS plots of spleen and liver cells from mice of the indicated genotypes on day 6 after tamoxifen treatment. **(F)** Representative

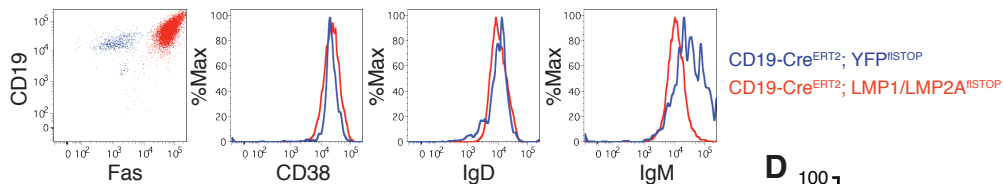
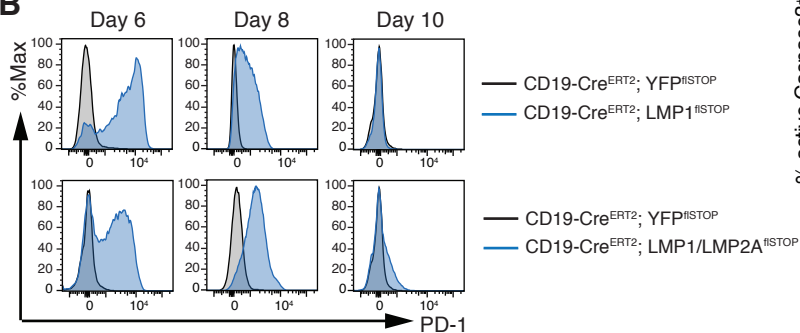
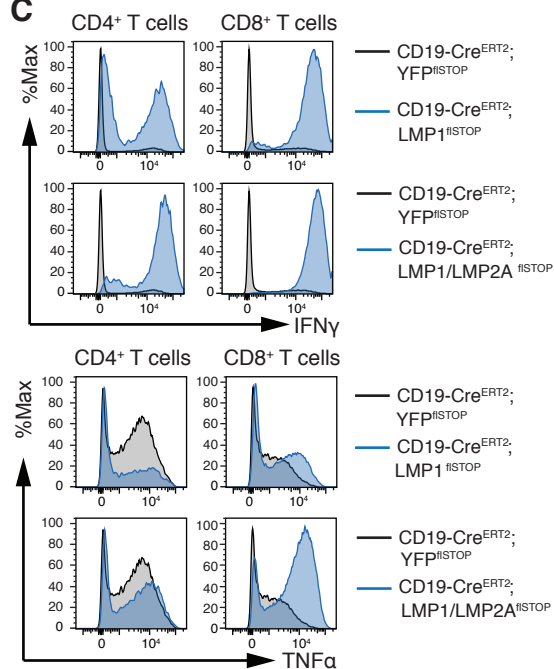
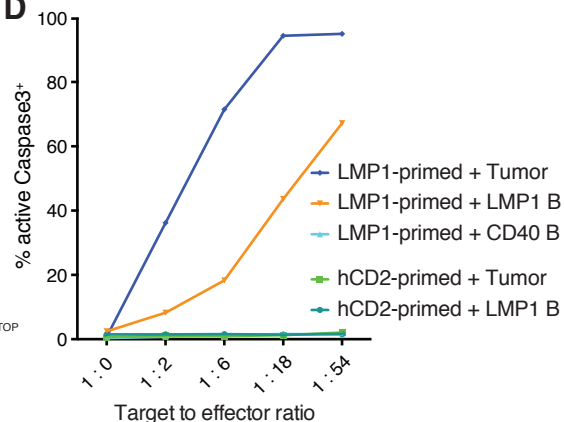
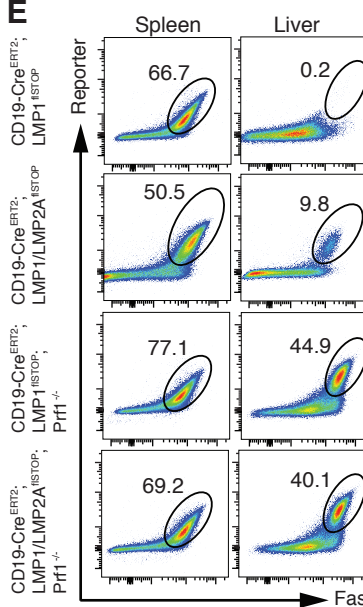
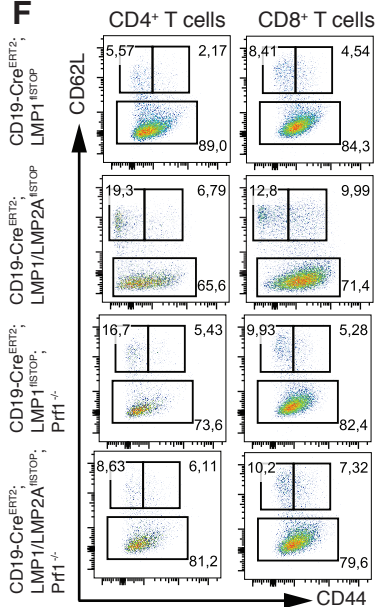
FACS plots of CD44 and CD62L surface expression on splenic T cells on day 6 after tamoxifen treatment..

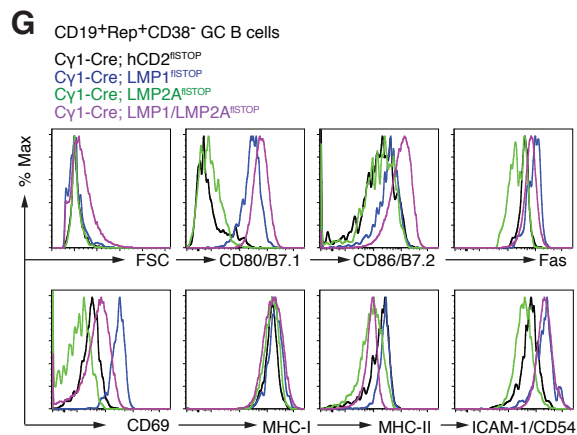
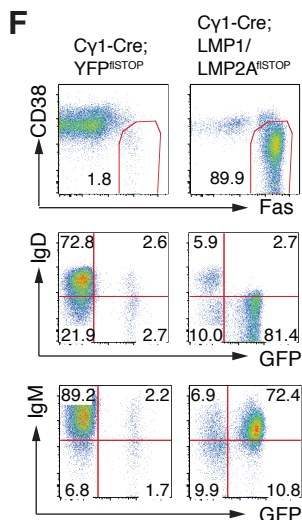
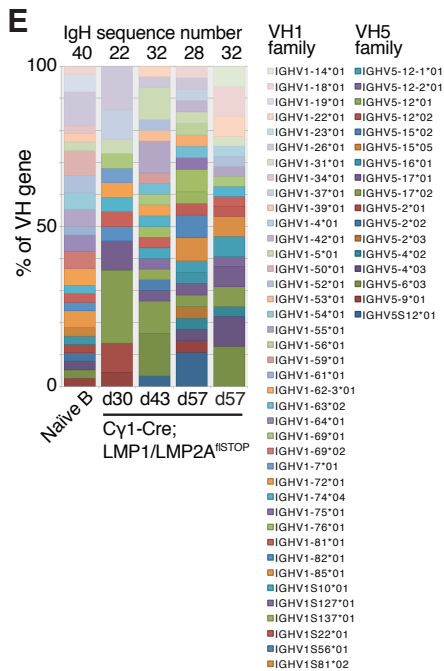
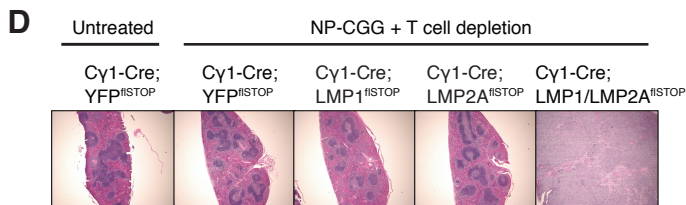
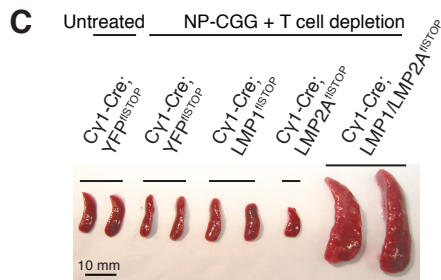
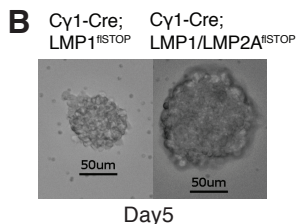
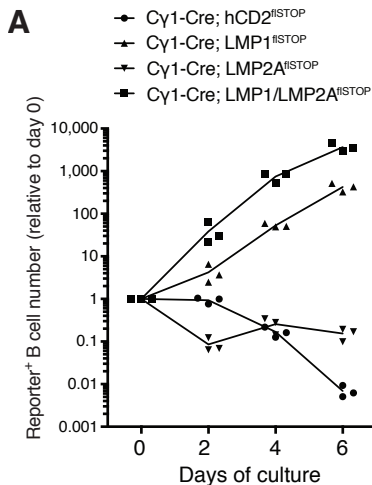
Figure S3. Conditional expression of LMP1 and LMP2A in GC B cells leads to fatal B cell expansion upon immunosuppressive treatment. **(A and B)** Splenic B cells were purified from mice with indicated genotypes and cultured in complete DMEM containing 10 % FCS and 2-Mercaptoethanol. Relative number of reporter⁺ B cells to day 0 are shown. Only cells expressing LMP1 or LMP1 and LMP2A proliferated and formed clusters as shown on representative microphotographs. **(C and D)** Mice of indicated genotypes were immunized with NP-CGG and treated with T cell-depleting antibodies on days 10, 17, 24, 31, 38, 45, and 52 after immunization and were sacrificed on day 57. Mice co-expressing LMP1 and LMP2A in GC B cells showed enlarged spleen (C) and a disturbed histological GC architecture in HE staining (D). **(E)** Expanded reporter⁺ cells of Cγ1cre; LMP1/LMP2A^{fSTOP} mice treated as in Fig. 4B were isolated on days 30, 43, and 57. IgH VH1 and VH5 family genes were amplified by PCR from genomic DNA and subjected to sequencing analysis. Frequencies of each VH gene within all analyzed sequences (VH1 plus VH5) are shown. **(F)** Splenocytes from mice treated as in C and D were analyzed by FACS for surface CD38, IgD, IgM, and Fas expression and for reporter expression (GFP/YFP). **(G)** Splenocytes from mice treated as in Fig. 4B were sacrificed on day 16 and analyzed by FACS for expression of surface receptors important for the interaction with T cells. Gated on CD19⁺Reporter⁺CD38⁻ cells. **(F and G)** Representative data for more than two independent experiments.

Figure S4. Conditional expression of LMP1 and LMP2A in GC B cells leads to T cell expansion, and constitutively active PI3K replaces LMP2A function. **(A)** Absolute numbers of αβ T, γδ T, and NK cells in spleens of mice from the experiment shown in Fig. 4C. **(B)** Splenic B cells stimulated with anti-IgM or anti-CD40, or expressing LMP1, LMP2A, or LMP1 and LMP2A were subjected to Western blot analysis of indicated signaling molecules. As controls, splenic B cells from C57BL/6 mice were stimulated by 10 μg/ml of anti-IgM or 5 μg/ml of anti-CD40 antibody for 3 min or 10 min. Splenic B cells from Cγ1cre; hCD2^{fSTOP}, Cγ1cre; LMP1^{fSTOP}, Cγ1cre; LMP2A^{fSTOP}, or Cγ1cre; LMP1/LMP2A^{fSTOP} mice were

stimulated with 2 $\mu\text{g/ml}$ of anti-CD40 and 25 ng/ml of mIL-4 for 3 days to induce transgene expression, then rinsed and cultured for additional 24 hours without stimulation prior to cell lysis. **(C)** Absolute numbers of $\alpha\beta$ T, $\gamma\delta$ T, and NK cells in spleens of mice from the experiment shown in Fig. 4F.

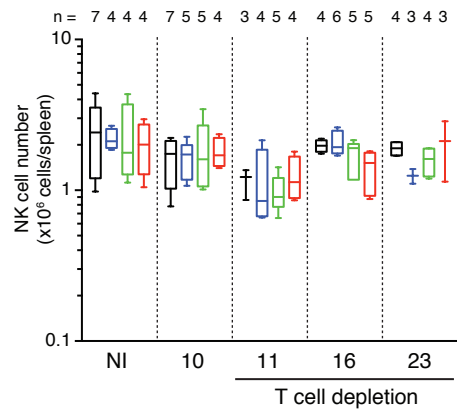
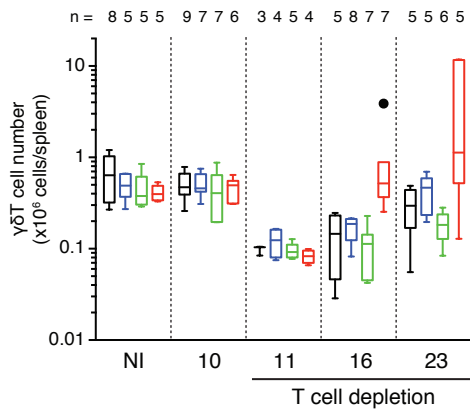
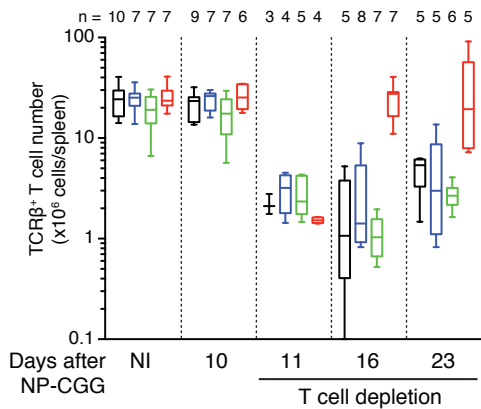
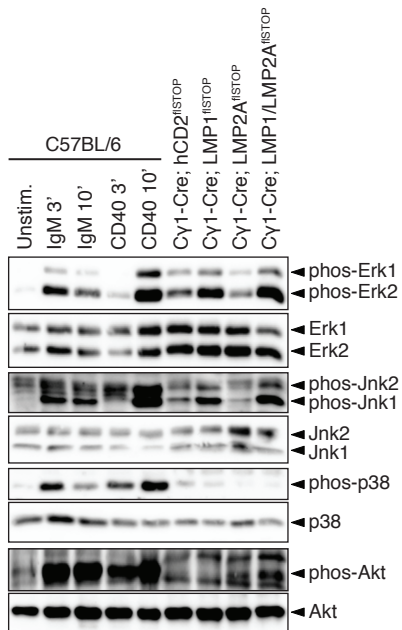


A**B****C****D****E****F**

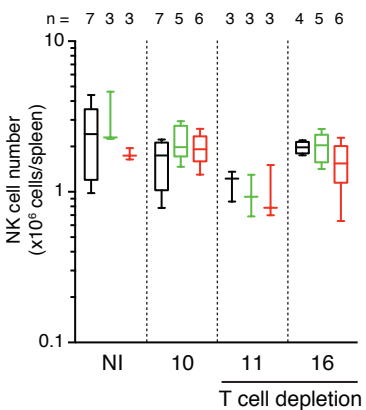
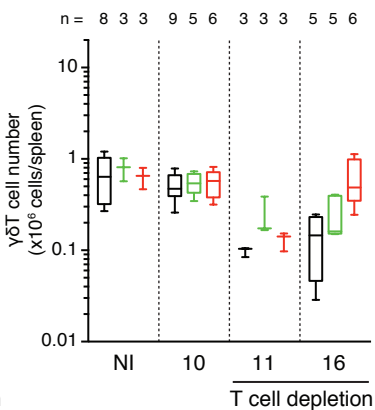
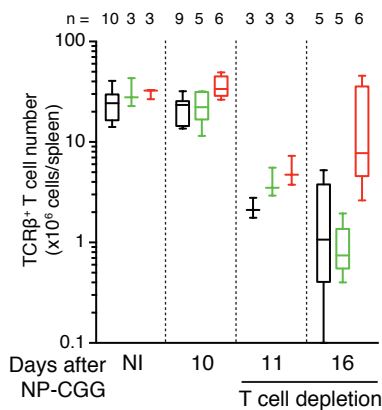


A

- Cy1-Cre; hCD2/YFP^{flSTOP}
- Cy1-Cre; LMP1^{flSTOP}
- Cy1-Cre; LMP2A^{flSTOP}
- Cy1-Cre; LMP1/LMP2A^{flSTOP}

**B****C**

- Cy1-Cre; hCD2/YFP^{flSTOP}
- Cy1-Cre; P110^{flSTOP}
- Cy1-Cre; LMP1/P110^{flSTOP}



Supplemental materials and methods

Flow Cytometry and Cell Sorting. Single cell suspensions were prepared in Dulbecco's modified Eagle's medium (DMEM) supplemented with 1% FCS and 1 mM EDTA, lysed red blood cells with Gey's solution, and cell numbers were counted. Cells were stained with the following Abs coupled to FITC, phycoerythrin (PE), peridinin chlorophyll (PerCP), PerCP-Cy5.5, allophycocyanin (APC), Alexa647, Alexa700, PE-Cy7, Pacific Blue, Pacific orange, Brilliant violet (BV) 421, BV510, BV605, BV650, BV711, or BV785: CD19, B220, GL-7, Fas, CD38, CD138, IgD, IgM, hCD2, CD80, CD86, H2-K^b, I-A/I-E, CD54 (ICAM-1), CD3 ϵ , TCR β , CD4, CD8a, CD62L, CD44, PD-1, $\gamma\delta$ TCR, NK1.1, DX5, CD69, IFN γ , TNF α , Active Caspase-3 purchased from Affymetrix eBioscience, BD Biosciences, or BioLegend. Samples were acquired on an LSRFortessa (BD Biosciences) and analyzed with FlowJo software (TreeStar). Cell sorting was done on a FACSARIA II (BD Biosciences). For intracellular cytokine staining, spleen cells from tamoxifen-treated CD19-Cre^{ERT2}; YFP^{fSTOP}, CD19-Cre^{ERT2}; LMP1^{fSTOP}, or CD19-Cre^{ERT2}; LMP1/LMP2A^{fSTOP} mice were cultured in the presence of 20 ng/ml PMA (Sigma), 2 μ g/ml Ionomycin (Sigma), 2 μ M Monensin (BioLegend), and 5 μ g/ml Brefeldin A (BioLegend) for 6 hrs at 37°C. After surface staining for TCR β , CD4, CD8a, and CD19, cells were fixed with 2% paraformaldehyde, permeabilized with 0.5% Saponin, and stained for IFN γ and TNF α .

***In vitro* cell culture.** Splenic B cells were enriched by depletion of CD43⁺ cells with anti-CD43 microbeads (Miltenyi Biotech). MACS purified B cells were cultured in DMEM supplemented with 10% FCS, 2 mM L-Glutamine, 1 mM Sodium Pyruvate, 10 mM HEPES, 52 μ M β -mercaptoethanol, Non-essential amino acids, penicillin, and streptomycin for 3 days. LMP1-expressing tumor cell lines were maintained in 15% FCS DMEM instead of 10% FCS.

Western blot analysis. CD43-depleted splenic B cells from C57BL/6 mice were stimulated with 10 μ g/ml anti-IgM F(ab')₂ (Jackson Immuno Research Laboratory) or 5 μ g/ml anti-CD40 (HM40-3; BD Biosciences) for indicated times. CD43-depleted splenic B cells from C γ 1cre; hCD2^{fSTOP}, C γ 1cre; LMP1^{fSTOP}, C γ 1cre; LMP2A^{fSTOP}, or C γ 1cre; LMP1/LMP2A^{fSTOP} mice were cultured for 3 days

in the presence of 2 µg/ml of anti-CD40 and 25 ng/ml of mouse IL-4 (Peprotech) for 3 days to induce transgene expression, then rinsed and cultured for additional 24 hours without stimulation prior to cell lysis. Cells were lysed with NP40 lysis buffer (1% NP40, 10 mM Tris, 150 mM NaCl, 0.5 mM EDTA, 10 mM NaF, 2 mM PMSF, 1 mM Sodium Orthovanadate, 10 µM Sodium Molybdate, and Complete mini protease inhibitor cocktail (Roche)). Whole cell lysates from B cells were separated on a 8.2 % polyacrylamide gel and transferred to a PVDF membrane (Millipore). The membrane was immunoblotted with the antibodies to phospho-Erk (T202/Y204), Erk1/Erk2, phospho-Jnk, Jnk, phospho-p38, p38, phospho-Akt (S473), or Akt from Cell Signaling Technology.

Bone marrow reconstitution. Rag2^{-/-}γC^{-/-} recipient mice were irradiated with a dose of 600 rad followed by i.v. injection of 2.5x10⁵ donor bone marrow cells. MACS-depletion of Thy1.2⁺, B220⁺, CD19⁺ cells from postnatal day 3 mouse bone marrow cells was performed to prepare donor HSCs. Recipients were given 0.16% neomycin-sulfate (Sigma) in their drinking water for 2 days prior to i.v. and 2 weeks after the donor cell transfer.

Somatic mutation analysis. Genomic DNA was prepared from sorted B cells of NP-CGG-immunized animals and the analysis was performed by published procedures (27-29). JH4 intron sequences obtained from animals harboring the Cy1cre allele have mixed C57BL/6 and 129P2 origin. Therefore, the origin of each sequence was first determined using nucleotide BLAST.

***In vitro* killing assay.** *In vitro* killing assay was performed as described previously (21). In brief, CD8 T cells from tamoxifen-treated CD19-Cre^{ERT2}; hCD2^{flSTOP} or CD19-Cre^{ERT2}; LMP1^{flSTOP} were purified by FACS sorting after MACS enrichment (Pan T cell isolation kit II, Miltenyi Biotec). T cells were incubated with various target cells at different effector:target ratios for 4 hr in 96-well plates, followed by intracellular active Caspase-3 staining (BD Biosciences). Murine LMP1-expressing tumor cell line was established from B cell lymphoma developed in Rag2^{-/-} mice transferred with Cy1-Cre; LMP1/LMP2A^{flSTOP} splenic B cells. MHC-I^{-/-}, MHC-II^{-/-}, and MHC-I^{-/-}; MHC-II^{-/-} sublines of LMP1 tumor cells were generated by Crispr/Cas9 mutagenesis using sgRNA complementary to

genes encoding β 2M or MHC-II I-A^b, and FACS sorting of MHC-I and/or II-deficient cells. Murine Burkitt lymphoma line was established from Rag2^{-/-} γ C^{-/-} mice reconstituted with C γ 1-Cre; Myc/P110^{flSTOP} BM cells (24). LMP1 B cells were prepared by *in vitro* TAT-Cre treatment of LMP1^{flSTOP} splenic B cells (21). CD40 B cells were prepared by anti-CD40 stimulation of LMP1^{flSTOP} splenic B cells. In all killing assays, effector-target mixtures in U-bottom 96-well plates were spun at 200 rpm for 2 min before moving to incubator, and cultures were stained for TCR β , CD4, CD8a, hCD2 and CD19 to identify target and effector cells. Active Caspase-3⁺ target cells represent apoptotic target cells.